ChemPhysMater 3 (2024) 230–238

Contents lists available at ScienceDirect

ChemPhysMater

journal homepage: https://www.keaipublishing.com/en/journals/chemphysmater/

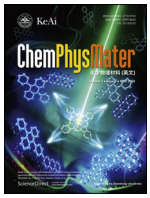

Research Article

Molecular origin for pH-responsive wormlike micelles of zwitterionic surfactants triggered by aromatic acid derivatives

Shuo Lu, Yonghang Cheng, Jinfeng Dong*, Xuefeng Li*

Engineering Research Center of Organosilicon Compounds & Materials, Ministry of Education, College of Chemistry and Molecular Sciences, Wuhan University, Wuhan 430072, China

ARTICLE INFO

Keywords:
Zwitterionic surfactants
Aromatic acid derivatives
pH response
Wormlike micelles
Spherical micelles
Viscosity

ABSTRACT

Introduction of aromatic acid derivatives (AADs) into zwitterionic surfactants is an efficient method to prepare wormlike micelles with pH-controllable viscosity; however, the coincident molecular origin of AAD/zwitterionic surfactant binary mixtures remains unclear. Herein, the self-assembly of hydroxyl derivatives of benzoic acid (BA) and cetyldimethyl betaine (BS-16) mixtures in water was systematically assessed, and various factors, such as the molecular structure, molar ratio of AAD and BS-16, and solution pH, were investigated. The structure–property relationship of AAD/BS-16 binary mixtures was established, which provided the molecular origin for the effect of AAD on micellar microstructures and the pH-induced morphological transitions. The ortho-substituted hydroxyl moiety in the BA molecule facilitated the formation of larger wormlike micelles, whereas the effect of the meta-substituted moiety was less significant. The para-substituted hydroxyl moiety in BA did not favor micellar growth. This moiety exhibited similar characteristics to the increasing hydroxyl moiety number in the AAD molecules or solution pH where the negative effects of steric hindrance and electrostatic interactions of molecules in micelles are dominant.

1. Introduction

The primary characteristics of surfactants are interfacial adsorption and the formation of self-organized aggregates within the bulk. These are also the foundation for the applications of surfactants, such as petrochemical engineering, pharmaceutical formulation, personal care, and nano-/micromaterial fabrication [1]. Wormlike micelles, one of the morphologies of surfactant aggregates, have contour lengths ranging from nanometers to micrometers in the longitudinal dimension [2–4]. These aggregates provide surfactant solutions with viscoelasticity similar to that of polymer solutions. Therefore, surfactant wormlike micelles have significant potential as replacements for polymer flooding agents in enhanced oil recovery (EOR) [5,6]. In addition, surfactant wormlike micelles are superior to polymers because they can simultaneously decrease crude oil/water interfacial tension. A recent study demonstrated that hybrid wormlike micelles composed of erucyl amidepropyl betaine (EAPB) and sodium dodecyl sulfate (SDS) had higher EOR efficiencies than partially hydrolyzed polyacrylamide with the same viscosity [7,8].

Generally, zwitterionic surfactants are the most suitable for EOR because of their excellent resistance to salinity, temperature, and adsorption onto rocks [9]. However, excluding those with very long hydrophobic tails such as EAPB, zwitterionic surfactants often only form spherical micelles [10–12]. The introduction of anionic surfactants or aromatic hydrotropes can significantly facilitate the formation of wormlike zwitterionic micelles. A recent study by Lu et al. showed that the viscosity of anionic/zwitterionic surfactant hybrid mixtures composed of sodium alkyl sulfate (SAS) and alkyl dimethyl amidopropyl hydroxyl sulfobetaine (AHSB) significantly increased by altering the hydrophobic chain length [13,14]. This provided a simple method for controlling the microstructural and viscoelastic characteristics of SAS/AHSB wormlike micelles. To date, many anionic/zwitterionic surfactant hybrid wormlike micelles have been developed based on the same technique [15–18]. Aromatic hydrotropes/zwitterionic surfactant hybrid wormlike micelles have also garnered significant attention. Additionally, cationic surfactant wormlike micelles have been developed using a similar approach [19–21]. These hybrid wormlike micelles exhibit excellent viscoelasticity and stimuli controllability because of the introduced hydrotropes [22,23].

The importance of aromatic hydrotropes in zwitterionic surfactants that can induce viscoelastic-to-gel-like wormlike micelle transitions was demonstrated by Raghavan et al. [24]. Similar gel-like wormlike micelles composed of octadecyl dimethyl amidopropyl hydroxyl sulfobetaine (OHSB) and sodium salicylate (NaSal) were developed recently. These wormlike micelles were transferred into spherical micelles

* Corresponding authors.
E-mail addresses: jfdong@whu.edu.cn (J. Dong), lixuefeng@whu.edu.cn (X. Li).

https://doi.org/10.1016/j.chphma.2024.02.002
Received 27 December 2023; Received in revised form 25 February 2024; Accepted 25 February 2024
Available online 12 March 2024
2772-5715/© 2024 The Authors. Publishing Services by Elsevier B.V. on behalf of KeAi Communications Co. Ltd. This is an open access article under the CC BY license (http://creativecommons.org/licenses/by/4.0/)

through the addition of amino compounds [25]. Generally, the type, position, and form of the polar moiety in the aromatic ring are critical for viscosity enhancement. These moieties determine the microenvironment of additives within aggregates, in the palisade layer, or in the micellar core. This microenvironment is attributed to the electrostatic interactions between the surfactants and additives [26]. The effects of carboxyl- and hydroxyl-substituted benzoate salts on zwitterionic surfactant wormlike micelles showed that all hydrotropes facilitated micellar growth and enhanced viscosity. Furthermore, the ortho-substituted salt was the most efficient, highlighting the structural importance of hydrotropes [27,28]. However, the pH-induced viscosity changes observed in the EAPB system (thickening) contradicted that of the oleyl amidopropyl betaine (OAPB) system (thinning). In both systems, the pH-induced changes in hydrogen and electrostatic interactions within the micelles were similar. Studies have demonstrated promising and diversified behaviors of hydrotropes/zwitterionic surfactant hybrid wormlike micelles [24–28]. However, an understanding of the coincident molecular origin of aromatic hydrotropes is limited.

In this study, a common zwitterionic surfactant, cetyldimethyl betaine (BS-16, Table 1), was employed to prevent hydrogen interactions between the amide moiety of the surfactants and the polar moiety of the hydrotropes in the micellar core. In addition, eight hydroxyl-substituted aromatic acid derivatives (AAD; Table 1), which were assessed for their hydroxyl moiety position and number, were used as hydrotropes. In these binary systems, the effects of surfactant composition, structure, and hydrotrope form on micellar structures, as well as the properties of the micelles were examined using steady rheological responses and cryogen transmission electron microscopy (cryo-TEM) measurements. The molecular interactions between the surfactants and hydrotropes were investigated using zeta potential and proton nuclear magnetic resonance (^{1}H NMR) techniques. Based on the established structure–property relationships, the molecular origin of the pH-responsive hydrotrope/zwitterionic surfactant hybrid wormlike micelles was clarified. These findings provide detailed information on stimuli-responsive hybrid wormlike micelles, which may also shed light on the smart control of fluid viscoelasticity.

2. Experimental section

2.1. Materials

The zwitterionic surfactant, BS-16, was synthesized and purified according to a previously reported method [29]. The structure was characterized using ^{1}H NMR and electrospray ionization mass spectrometry (ESI-MS) (Supporting Information, Figs. S1 and S2). Aromatic acid derivatives, including benzoic acid (AR), 2-hydroxybenzoic acid (AR), 3-hydroxybenzoic acid (98%), 4-hydroxybenzoic acid (99%), 2,3-dihydroxybenzoic acid (98%), 2,4-dihydroxybenzoic acid (98%), 2,5-dihydroxybenzoic acid (98%), 2,6-dihydroxybenzoic acid (98%), 3,4-dihydroxybenzoic acid (98%), and 3,5-dihydroxybenzoic acid (98%), were purchased from Aladdin (Shanghai, China) and used as received. All other chemicals used in this study were analytically pure, purchased from Sinopharm Chemical Reagent Co., Ltd. (Shanghai, China), and used as received. Ultrapure water (18.2 MΩ cm at 25 °C) was produced using a Millipore-Q system.

2.2. Samples preparation

All AAD/BS-16 samples were prepared by mixing stock solutions of BS-16 and AAD with stirring at 60 °C until homogeneous. Subsequently, the solution pH of each sample was adjusted using 0.5 M NaOH or 0.5 M HCl aqueous solutions. The pH measurements were conducted using the PB-10 pH meter (Sartorius, Germany). All samples were equilibrated at 25 °C for a minimum of 24 h prior to analysis.

2.3. Characterization methods

2.3.1. Steady rheological measurements

Steady rheological measurements were performed by a HAAKE MARS 60 rheometer (ThermoFisher Scientific, Germany) using a Couette geometry DG 41 at 25 °C. The samples were equilibrated for a minimum of 10 min prior to each measurement.

Table 1
Molecular structures of BS-16 and AAD.

BS-16	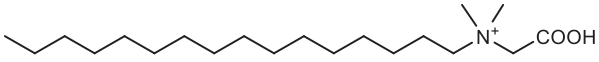		
AAD	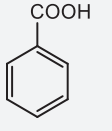 BA	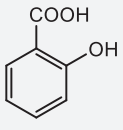 2-HBA	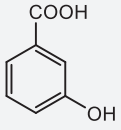 3-HBA
	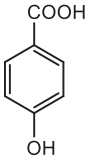 4-HBA	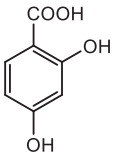 2,4-DHBA	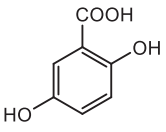 2,5-DHBA
	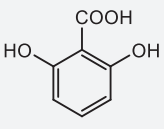 2,6-DHBA	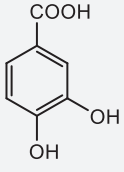 3,4-DHBA	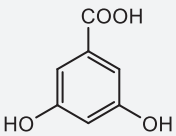 3,5-DHBA

2.3.2. Cryo-TEM measurements

The cryo-TEM specimens were prepared as follows: First, 2 μL of test solution was dropped on a TEM copper grid covered with a holey carbon film; excess sample was blotted away to form a liquid film after 3 s. Subsequently, the grid was immediately plunged into liquid ethane, which was condensed using liquid nitrogen. This mixture remained in liquid nitrogen (−173 ˚C) until measurement. Finally, cryo-TEM images were obtained using a transmission electron microscope (JEOL 1400; Talos, USA) at an accelerating voltage of 200 kV under low-dose conditions.

2.3.3. ^1H NMR measurements

Samples for ^1H NMR spectra measurements were all prepared using D_2O. Spectral analysis was conducted using a 400 MHz Bruker-BioSpin spectrometer (Bruker, USA) at 25 °C.

2.3.4. Zeta potential measurements

Zeta potential measurements of aqueous samples were performed on a Zetasizer (ZEN 3600; Malvern, UK) with a 173˚ back scattering angle and He–Ne laser (λ = 633 nm) at 25 ˚C.

3. Results and discussions

3.1. Effect of the AAD on the self-assembly of BS-16 aqueous solutions

BS-16 formed spherical micelles in brine, whereas the introduced AAD facilitated a significant transition of spherical micelles to wormlike micelles. Therefore, AAD/BS-16 aqueous solutions were viscous, and the self-assembly behavior of the AAD/BS-16 mixtures were significantly affected by the molecular structure of AAD, the molar fraction of AAD ($x_{AAD} = c_{AAD}/(c_{BS\text{-}16} + c_{AAD})$) and solution pH. Fig. 1 shows images of the BA/BS-16, 2-HBA/BS-16 and 2,6-DHBA/BS-16 aqueous mixtures across different pH levels. The temperature, and concentrations of BS-16 ($c_{BS\text{-}16}$) and x_{AAD} remained constant at 25 ˚C, 10 mM and 0.5, respectively. General pH-induced transitions were observed in all three AAD/BS-16 systems. Depending on the type of AAD used, the AAD/BS-16 mixtures were bluish in color or formed precipitates at pH values below 4. However, the mixtures were homogeneous above the critical pH of each AAD/BS-16 system. Moreover, the transparent samples were viscous within the 4–5 pH range, whereas the samples were aqueous in consistency at higher pH values. This suggests that the pH of the solution induced the transition from wormlike micelles to spherical micelles [30]. Similar transitions were also observed in other AAD/BS-16 systems (Table 1). However, the pH region at which the AAD/BS-16 samples exhibited viscosity was dependent on the AAD used.

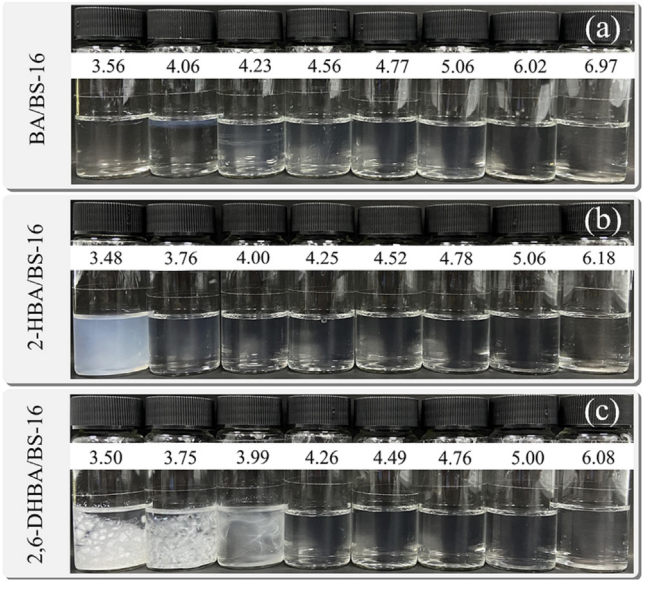

Fig. 1. Images of BA/BS-16 (a), 2-HBA/BS-16 (b) and 2,6-DHBA/BS-16 (c) aqueous solutions at constant $c_{BS\text{-}16}$(10 mM) and x_{AAD} (0.5), and varying pH values.

3.2. Aggregation behaviors of 2-HBA/BS-16 aqueous mixtures

The self-assembly behaviors of all AAD/BS-16 systems were mainly affected by x_{AAD} and pH. The 2-HBA/BS-16 aqueous mixture was examined to quantify the importance of x_2-HBA and pH when $c_{BS\text{-}16}$ remained constant at 10 mM. Fig. 2(a) shows the shear viscosity of 2-HBA/BS-16 aqueous solutions at constant x_2-HBA (0.5) and varying levels of pH. Under acidic conditions, the viscosities and shear-thinning characteristics of 2-HBA/BS-16 aqueous solutions were similar to those of wormlike micelles [13]. The viscosities of the 2-HBA/BS-16 solutions were significantly reduced at pH values of 4.8 and 5.1. At these pH values, minimal shear-thickening behaviors were observed, which are often caused by the shear-induced allies of wormlike micelles [13]. At pH = 7.1, the viscosities were similar to that of water (~1 mPa s), indicating that spherical micelles were formed. A pH-dependent zero-shear viscosity (η_0) was exhibited by the pH-induced reduction in viscosity (the inset image of Fig. 2(a)). The η_0 value of the 2-HBA/BS-16 aqueous solutions decreased by approximately 10^3-fold as the pH increased from 4 to 5.

Fig. 2(b) shows the steady rheological responses of 2-HBA/BS-16 aqueous solutions at pH = 4.3 and varying x_2-HBA values. At an x_2-HBA value of 0.1, the viscosity remained low, similar to that of the pure BS-16 aqueous solution. The viscosities of the 2-HBA/BS-16 aqueous solutions increased with an increase in x_2-HBA. These solutions exhibited the shear-thinning characteristics of wormlike micelles at higher x_2-HBA values. The x_2-HBA-dependent zero-shear viscosity is shown in the top-right image of Fig. 2(b). At x_2-HBA values lower than 0.25, a marginal increase in the η_0 values of 2-HBA/BS-16 aqueous solutions were observed. Between x_2-HBA values of 0.25 to 0.55, η_0 increased by approximately 10^3-fold. This indicated that the growth of wormlike micelles was induced by the continuous introduction of 2-HBA. At an x_2-HBA of 0.75, the zero-shear viscosity of the sample remained relatively constant. The viscosity results of the 2-HBA/BS-16 aqueous mixtures confirmed the pH- and x_2-HBA-induced formation of wormlike micelles.

Fig. 3 shows the cryo-TEM images of the 2-HBA/BS-16 samples at different x_2-HBA and pH values. For the 2-HBA/BS-16 samples at pH 4.3, long, flexible, and entangled wormlike micelles were observed at x_2-HBA values of 0.1 (Fig. 3(a)), 0.5 (Fig. 3(b)) and 0.67 (Fig. 3(c)), respectively. The main difference between the samples was the quantity of visible wormlike micelles. The higher the x_2-HBA level, the higher the fraction of wormlike micelles. This highlights the significance of 2-HBA in facilitating the growth of wormlike micelles, and the mechanism of increasing viscosity induced by x_2-HBA (Fig. 2(b)). The 2-HBA/BS-16 sample with a higher x_2-HBA content, exhibited a relatively higher viscosity.

Fig. 3(d) shows a cryo-TEM image of the 2-HBA/BS-16 aqueous solution at pH and x_2-HBA values of 7.0 and 0.5, respectively; mainly spherical micelles are visible. This confirmed the pH-induced transition of the wormlike micelles (Fig. 3(c)) to spherical micelles. In general, the cryo-TEM results were consistent with the steady rheological responses of the 2-HBA/BS-16 samples (Fig. 2(a)). Therefore, the x_2-HBA-induced viscosity increase of the 2-HBA/BS-16 samples at pH = 4.3 was attributed to the formation of long and entangled wormlike micelles; additionally, increasing x_{AAD} also enhanced viscosity because of the enlarged fraction of wormlike micelles. Alternatively, the pH-induced reduction in viscosity of the 2-HBA/BS-16 samples was caused by morphological changes from wormlike to spherical micelles.

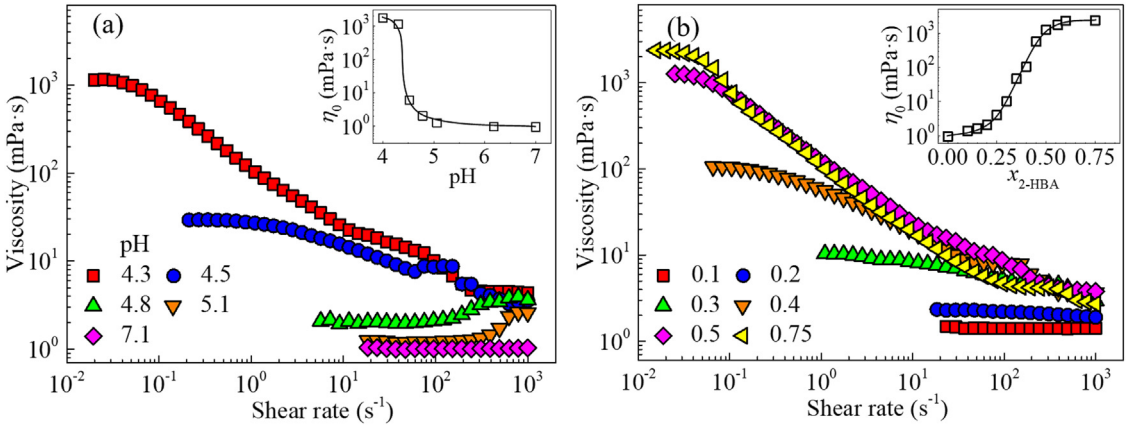

Fig. 2. The steady rheological responses of 2-HBA/BS-16 aqueous solutions at constant $c_{BS\text{-}16}$ (10 mM) and temperature (25 °C). The responses of the solutions were assessed at varying pH values and a constant x_2-HBA of 0.5 (a), and varying x_2-HBA and a constant pH of 4.3 (b). The inset in each panel represents the corresponding variation in zero-shear viscosity.

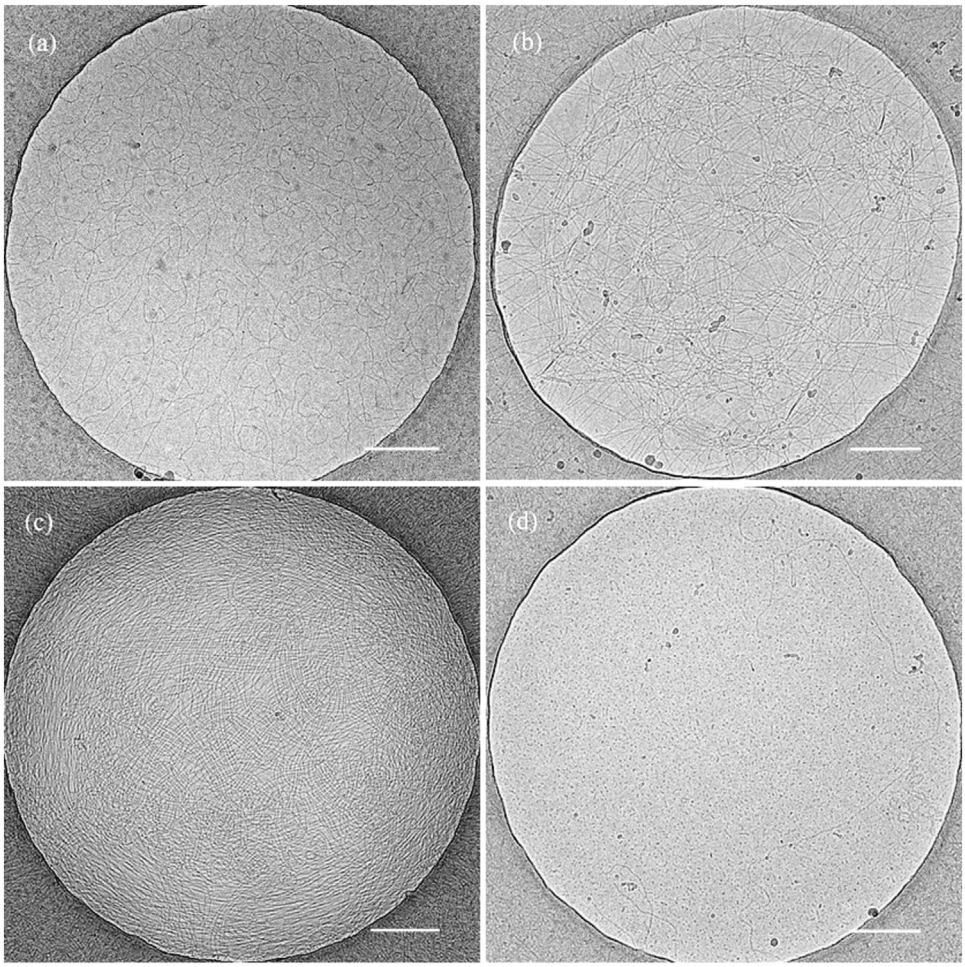

Fig. 3. Cryo-TEM images of the 2-HBA/BS-16 samples under varying conditions: x_2-HBA of 0.1 (a), 0.5 (b), and 0.67 (c) at pH = 4.3, and x_2-HBA of 0.5 at pH = 7.0 (d). Bars represent a magnification of 200 nm.

3.3. General self-assembly characteristics of AAD/BS-16 systems

3.3.1. Effects of AAD molecular structures

Figs. 4(a)(b) show the steady rheological responses of the AAD/BS-16 samples at constant $c_{BS\text{-}16}$, x_{AAD}, and pH values of 10 mM, 0.5, and 4.3, respectively. The viscosity of the BS-16 aqueous solution was significantly enhanced by the introduced AAD. In addition, the rheological responses of the AAD/BS-16 hybrid samples exhibited shear-thinning characteristics, except for that of the 3,5-DHBA/BS-16 mixture, which was attributed to the wormlike micelles. This verified the generality of AAD-induced transitions from spherical micelles to wormlike micelles in AAD/BS-16 aqueous solutions. However, the efficiency of AAD in inducing the formation of wormlike micelles was highly dependent on its molecular structure—the number and location of the hydroxyl moieties

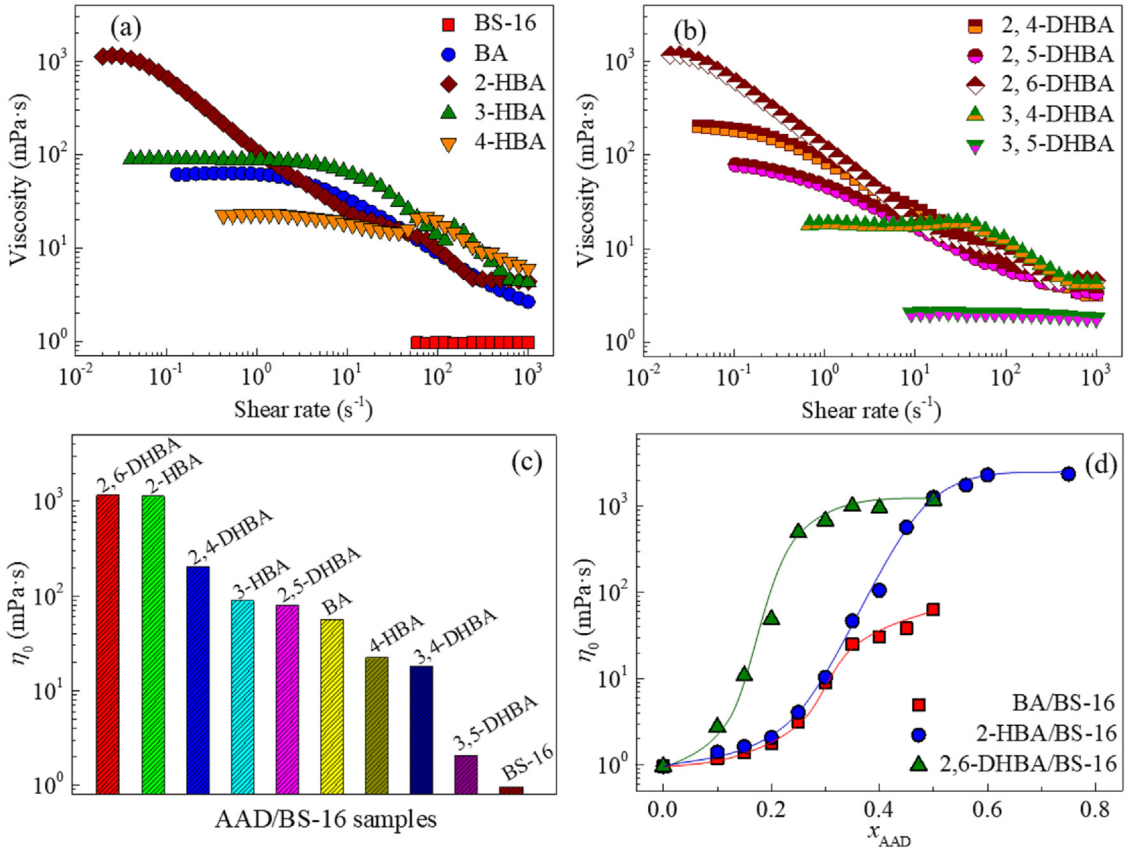

Fig. 4. The effect of AAD on the steady rheological responses (a)(b) and zero-shear viscosity (c) of 10 mM BS-16 aqueous solutions at pH = 4.3 and an x_{AAD} of 0.5. The x_{AAD}-dependent zero-shear viscosity (d) of 10 mM BS-16 aqueous solutions at pH = 4.3 is also shown.

in the aromatic ring. This was demonstrated by the variational zero-shear viscosities (Fig. 4(c)).

In terms of the molecular structure, BA was the key unit of all AAD molecules. The BA/BS-16 mixture exhibited an intermediate η_0 value, highlighting the importance of the number and location of the hydroxyl moiety of AAD molecules in hybrid micellar microstructures. Because η_0 values decreased in the order of 2-HBA/BS-16 > 3-HBA/BS-16 > BA/BS-16 > 4-HBA/BS-16, the location function of the introduced hydroxyl moiety in the BA molecule could have been evaluated. Compared with the finite contribution of the meta-substituted hydroxyl moiety, the ortho-substituted moiety was beneficial for the formation of larger wormlike micelles. In contrast, the para-substituted hydroxyl moiety had the opposite effect, resulting in smaller wormlike micelles and a lower viscosity. In addition to the electrostatic interactions between the HBA and BS-16 molecules, the function of aromatic hydrotropes in inducing micellar growth was mainly attributed to hydrophobic interactions between the tail of the surfactant and the aromatic ring in the hydrophobic section of the aggregates [23,31–33]. Therefore, the efficient insertion of hydrotropes in aggregates was the main factor. This insertion increased the hydrophobic volume and resulted in the denser packing of molecules in aggregates because of the weakened electrostatic interactions.

For double-substituted AAD molecules (DHBA), including 2,6-DHBA, 2,5-DHBA, and 2,4-DHBA, an additional hydroxyl moiety was introduced at the ortho-, meta-, and para-positions of 2-HBA, respectively (Table 1). The η_0 values of these molecules decreased in the order of 2,6-DHBA/BS-16 > 2,4-DHBA/BS-16 > 2,5-DHBA/BS-16, which was similar to that of the HBA/BS-16 mixtures. An additional hydroxyl moiety was generally disadvantageous for the formation of larger wormlike micelles; the meta-hydroxyl moiety remained the most pronounced. The η_0 values of the DHSB/BS-16 systems were generally lower than that of 2-HBA/BS-16. This difference was attributed to the steric hindrance between the DHBA and BS-16 molecules. For example, the symmetrically distributed hydrophilic moieties of 2,5-DHBA hinder its efficient insertion into the hybrid aggregates. Accordingly, the molecules were loosely packed, favoring smaller wormlike micelles. The disadvantage of this steric hindrance was observed in the 3-HBA/BS-16, 3,4-DHBA/BS-16 and 3,5-DHBA/BS-16 mixtures. The η_0 values followed the order of 3-HBA/BS-16 > 3,4-DHBA/BS-16 > 3,5-DHBA/BS-16. The presence of multiple hydroxyl moieties at any position within AAD molecules limited the formation of larger wormlike micelles because of steric hindrance. This corroborates the results of a previous study [22].

The effect of x_{AAD} on AAD/BS-16 micellar viscosity was also assessed (Supporting Information Fig. S3). Figs. 3(d) shows the x_{AAD}-dependent zero-shear viscosities of BA/BS-16, 2-HBA/BS-16 and 2,6-DHBA/BS-16 at pH = 4.3. For each system, an increase in x_{AAD} resulted in an increase in η_0 until the solubility limit of AAD was reached. However, differences in the efficiency of AAD molecules remained. For example, the maximum η_0 of the BA/BS-16, 2-HBA/BS-16, and 2,6-DHBA/BS-16 mixtures at x_{BA} = 0.5 were 63 mPa s, and approximately 2400 mPa s and 1200 mPa s, respectively. This confirmed that the presence of a hydroxyl moiety improved the growth of wormlike micelles; however, the introduction of additional hydroxyl moieties is disadvantageous. Moreover, the critical x_{AAD} that facilitates the maximum viscosity of the 2-HBA/BS-16 and 2,6-DHBA/BS-16 samples were approximately 0.5 and 0.2, respectively. This suggests that the higher efficiency of 2,6-DHBA in facilitating micellar growth and its relatively larger molecular volume may be the main causes in comparison with that of 2-HBA.

3.3.2. *Effects of pH*

In addition to the structural effects of the AAD molecules, the viscosities of the AAD/BS-16 aqueous mixtures were also affected by pH

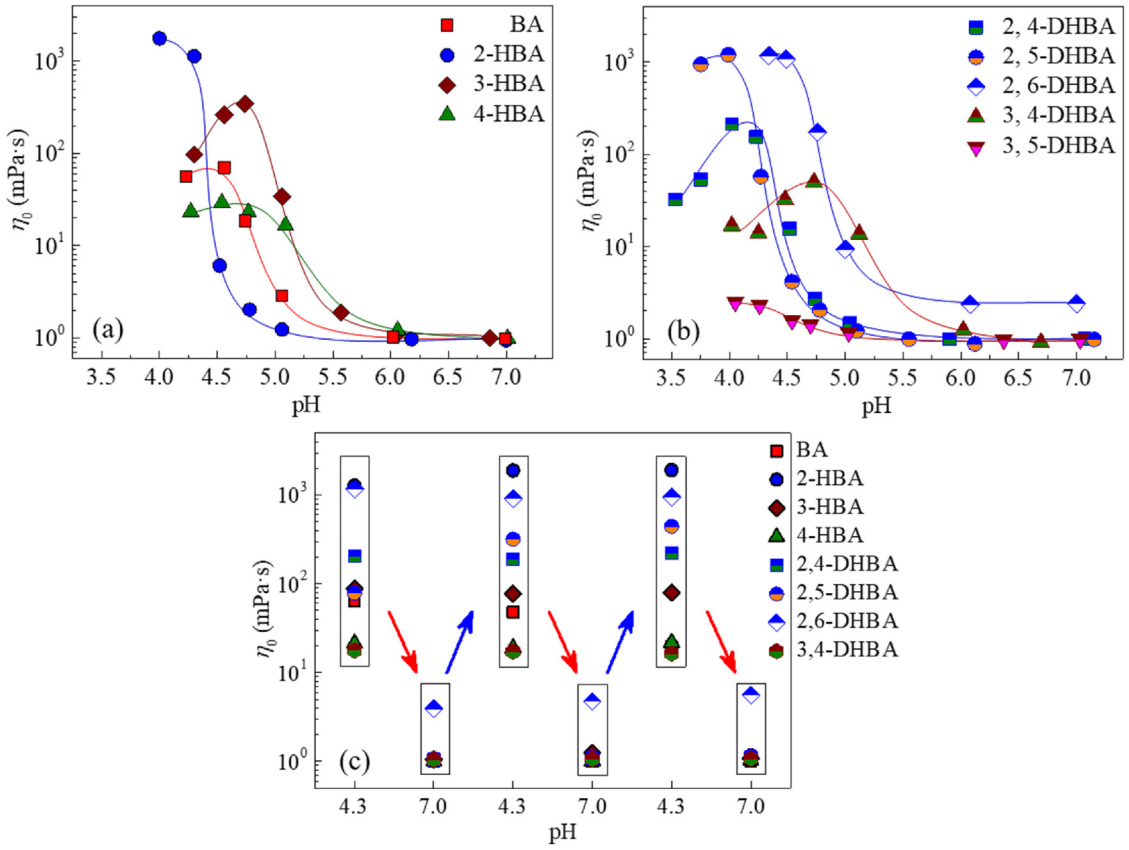

Fig. 5. The effect of pH on the zero-shear viscosities (a)(b) of AAD/BS-16 aqueous solutions at $c_{BS\text{-}16}$ = 10 mM and x_{AAD} = 0.5. The pH-induced reversible transitions are shown in (c).

(Supporting Information Fig. S4). Figs. 4(a)(b) show the pH-dependent η_0 of AAD/BS-16 aqueous solutions. In general, the η_0 of each AAD/BS-16 series decreased within a pH range of approximately 4.0 to 5.5. These values remained almost constant at higher pH levels. The steady rheological responses of all AAD/BS-16 aqueous solutions at low pH values, such as pH 4.5, exhibited shear-thinning behaviors with relatively high η_0 values. These characteristics are typical for long and entangled worm-like micelles [13,14].

After the solution pH was adjusted to neutral (generally above pH = 5.5), the viscosities of AAD/BS-16 aqueous solutions were independent of the shear rate with very low η_0 values, suggesting that smaller spherical micelles were formed; this was confirmed using cryo-TEM (Fig. 3(d)). These results confirmed the pH-induced micellar transitions between different morphologies, thereby enabling the pH-adjustable viscosities of the AAD/BS-16 aqueous solutions. Fig. 5(c) shows the zero-shear viscosities of the AAD/BS-16 aqueous mixtures at $c_{BS\text{-}16}$ and x_{AAD} values of 10 mM and 0.5, respectively. These viscosities were measured after sustained pH regulation between pH = 4.3 and 7 using NaOH and HCl aqueous solutions. The η_0 value of all AAD/BS-16 aqueous solutions could be reversed at a given pH. Additionally, the specific rangeability of η_0 mainly depended on the employed AAD. Moreover, the η_0 of each sample at pH = 7 was significantly lower than those at pH = 4.3 because of the micellar growth under acidic conditions.

3.4. Molecular interactions between BS-16 and AAD

Fig. 6(a) shows the pH-dependent zeta potentials (ζ) of the BS-16 and 2-HBA/BS-16 aqueous solutions. Because of the preferentially bound anions, Cl^-, introduced during pH regulation, a marginal reduction of ζ from ~2 mV to −5 mV was observed as the pH increased in the BS-16 aqueous solution. This occurred because the ionic degree of the carboxyl moiety significantly increased as the pH increased from 4 to 5 (Fig. 6(b)), which was demonstrated by the ionic species distribution of BS-16 (pK_a = 4.5). At the same pH range, variations in the ζ value of 2-HBA/BS-16 hybrid micelles were more pronounced; these values decreased from approximately −10 to −40 mV, and then remained constant at the higher pH level. Although the increased content of ionized 2-HBA was fixed at ~10% (Fig. 6(b)), the enhanced ionic degree of the ammonium moiety in BS-16 could facilitate the binding of ionized 2-HBA in the hybrid micelles based on electrostatic interactions [27,28]. This resulted in the addition of more negative charges to the 2-HBA/BS-16 hybrid micelles, which resulted in a more negative zeta potential. The η_0 of most of the AAD/BS-16 samples were highest at a pH of approximately 4.5 regardless of the AAD employed (Fig. 5). Therefore, the pH-induced morphological transitions in the AAD/BS-16 aqueous mixtures were mainly caused by BS-16, which were attributed to the wide variations in the ionic degree of BS-16. The pH regulation marginally affected the pure BS-16 aqueous solution, highlighting the importance of the introduced AAD in the development of pH-responsive BS-16 micellar systems.

For improved understanding, the BA/BS-16, 2-HBA/BS-16 and 2,6-DHBA/BS-16 binary systems were further assessed using ^{1}H NMR spectroscopy (Supporting Information Figs. S5 and S6). Fig. 6(c) shows the chemical shift changes ($\Delta\delta = \delta_{AAD/BS\text{-}16} - \delta_{AAD}$) of specific aromatic protons at pH, x_{AAD} and $c_{BS\text{-}16}$ values for all samples of 4.3, 0.5 and 10 mM, respectively. $\Delta\delta$ was dependent on its location and marginally affected by the number of hydroxyl moieties. The chemical shifts of protons H3, H4 and H5 moved toward the low fields, resulting in a more negative $\Delta\delta$; the $\Delta\delta$ of proton H4 was the most significant of the three systems. Therefore, these protons should exist in a more apolar environment in

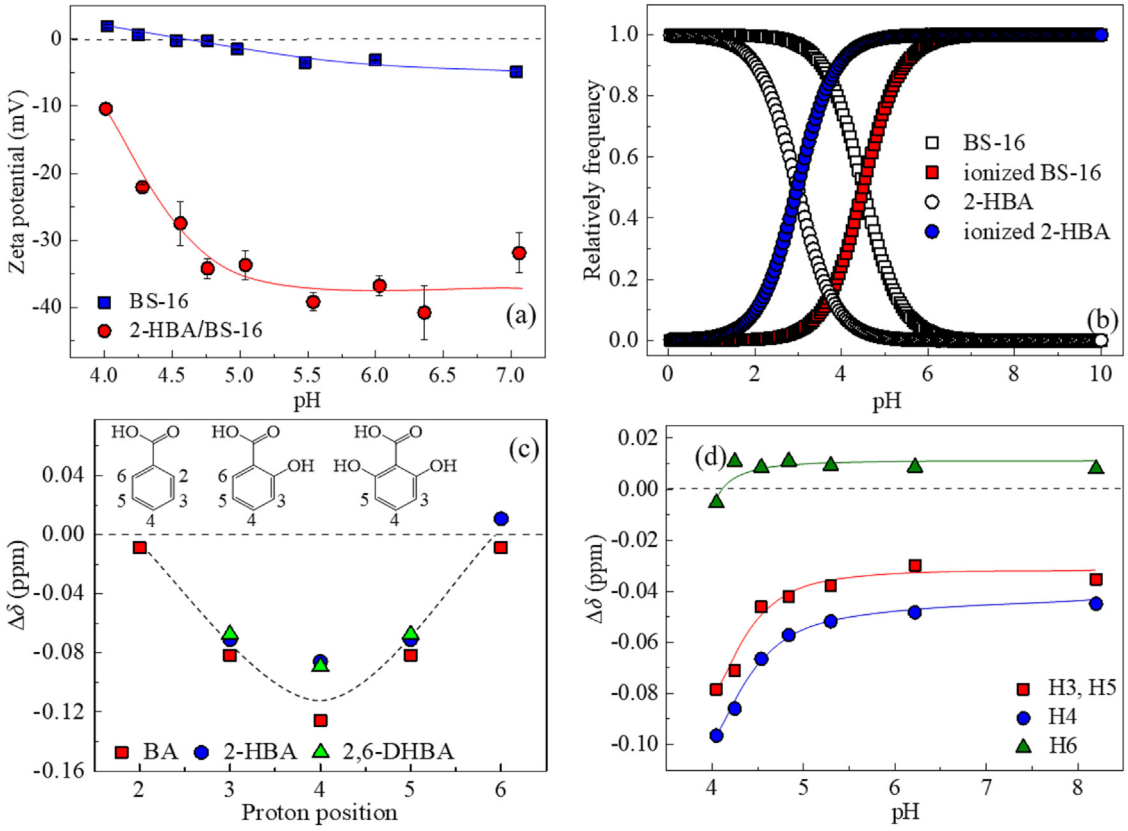

Fig. 6. pH-dependent distribution of ionic species (a), zeta potential (b), and chemical shift changes in AAD/BS-16 at constant (c) and varying (d) pH levels.

the micelles than in their molecular states. This indicates that the aromatic rings of AAD molecules were inserted into the hydrophobic micellar cores [22,23]. The deeper the insertion of the aromatic rings, the higher the $\Delta\delta$ value. However, the chemical shifts of protons H2 and H6 in the BA/BS-16 and 2-HBA/BS-16 hybrid micelles were marginally altered, indicating microenvironmental similarities in micelles and molecular states. This may be explained by their location in the polar palisade layer of the micelles.

The $\Delta\delta$ of each proton of the BA molecule was marginally higher than that of the corresponding proton in 2-HBA or 2,6-DHBA. This may be attributed to the increased steric hindrance between AAD and BS-16 (Fig. 4). The polar hydroxyl moieties in 2-HBA and 2,6-DHBA weakened the insertion efficiency of the aromatic rings in the micellar cores. The $\Delta\delta$ value of protons H3–H6 decreased as the pH of the 2-HBA/BS-16 aqueous mixtures increased from 4.3 to 6.0 (Fig. 6(d)). More polar microenvironments were observed at higher pH levels. This may be due to the looser packing manner of the 2-HBA and BS-16 molecules at higher pH levels. The increased ionization degrees of BS-16 and 2-HBA at higher pH levels are beneficial for the enhancement of electrostatic interactions between 2-HBA and BS-16 and facilitate the development of micelles with more polar palisade layers. Simultaneously, the BS-16 molecules in the hybrid micelles likely adopt a looser packing arrangement because of the increased electrostatic repulsion between molecules in the micelles at a higher pH (Fig. 6(a)). This also results in the formation of smaller micelles, which has been discussed in previous studies [32–36].

The effects of AAD and pH on the self-assembly behavior of the AAD/BS-16 hybrid systems are shown in Fig. 7. Generally, spherical micelles are formed in aqueous solutions of BS-16 under neutral conditions. The micellar morphologies were retained after the introduction of the AAD, regardless of the molecular structure. However, the morphologies of the AAD/BS-16 hybrid micelles were pH-sensitive. Spherical and wormlike micelles were formed under basic and acidic conditions, respectively; therefore, the pH-controllable viscosities of the AAD/BS-16 systems were achieved. The pH-induced formation of wormlike micelles was mainly attributed to the protonation of BS-16 under acidic conditions. However, the protonation of AAD was also beneficial, but less important. The number and location of hydroxyl moieties in the AAD molecules may affect the formation of wormlike micelles under acidic

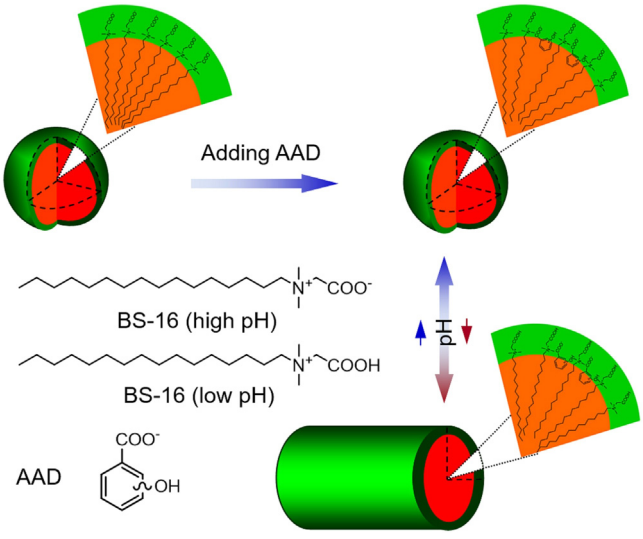

Fig. 7. The effects of AAD and pH on the morphology of AAD/BS-16 micelles.

conditions. This may have occurred because of the steric hindrance between BS-16 and AAD molecules.

4. Conclusions

This study systematically analyzed the micellization characteristics of binary mixtures composed of AAD and BS-16. The general role of AAD in inducing micellar growth in BS-16 micelles was elucidated. The effect of the molecular structure of AAD molecules on the formation of AAD/BS-16 hybrid wormlike micelles was determined. The AAD molecules participate in micellization by inserting aromatic rings into the micellar core. The electrostatic interactions between the carboxylate and ammonium moieties in the AAD and BS-16 molecules are important. Regarding the influence of the hydroxyl moiety in the AAD molecule on the formation of wormlike micelles, the position of the hydroxyl moiety in the aromatic ring has a stronger effect than its number. The ortho-substituted hydroxyl moiety in the BA molecule facilitated the formation of larger wormlike micelles, whereas the effect of the meta-substituted moiety was limited. However, the para-substituted moiety had numerous disadvantages. These differences were mainly due to the increased hydroxyl moieties in BA molecules (regardless of position) and the steric hindrance between the AAD and BS-16 molecules. Furthermore, pH-induced reversible transitions between wormlike and spherical micelles were observed, which were mainly attributed to the pH-induced ionization of the carboxyl moiety in BS-16. Finally, the electrostatic interactions between AAD and BS-16 were clarified. This study improves the understanding of the formation of betaine wormlike micelles enhanced by poly-hydroxy hydrotropes and aids in the development and application of responsive intelligent fluids.

Declaration of Competing Interest

The authors declare that they have no known competing financial interests or personal relationships that could have appeared to influence the work reported in this paper.

CRediT authorship contribution statement

Shuo Lu: Writing – original draft, Investigation, Formal analysis, Data curation. **Yonghang Cheng:** Investigation. **Jinfeng Dong:** Writing – review & editing, Supervision, Conceptualization. **Xuefeng Li:** Writing – review & editing, Supervision, Project administration, Funding acquisition, Conceptualization.

Acknowledgements

We acknowledge support from the National Natural Science Foundation of China [NSFC 22072109 and 22372125]. We are grateful to the Core Facility of Wuhan University for the cryo-TEM measurements.

Supplementary materials

Supplementary material associated with this article can be found, in the online version, at doi:10.1016/j.chphma.2024.02.002.

References

[1] S.M. Shaban, J. Kang, D. Kim, Surfactants: Recent advances and their applications, Compos. Commun. 22 (2020) 100537.
[2] S. Ezrahi, E. Tuval, A. Aserin, Properties, main applications and perspectives of worm micelles, Adv. Colloid Interface Sci. 128 (2006) 77–102.
[3] M. Liberatore, F. Nettesheim, P. Vasquez, M. Helgeson, N. Wagner, E. Kaler, L. Cook, L. Porcar, Y. Hu, Microstructure and shear rheology of entangled wormlike micelles in solution, J. Rheol. 53 (2009) 441–458.
[4] D. Danino, T. Zemb, On the shape and connections of micelles: Electron microscopy imaging inspiring thermodynamic modelling, Curr. Opin. Colloid Interface Sci. 61 (2022) 101607.
[5] F. Afolabi, S.M. Mahmood, N. Yekeen, S. Akbari, H. Sharifigaliuk, Polymeric surfactants for enhanced oil recovery: A review of recent progress, J. Pet. Sci. Eng. 208 (2022) 109358.
[6] S. Chowdhury, S. Shrivastava, A. Kakati, J.S. Sangwai, Comprehensive review on the role of surfactants in the chemical enhanced oil recovery process, Ind. Eng. Chem. Res. 61 (2022) 21–64.
[7] B. Zhou, W. Kang, Q. Wang, X. Li, Y. He, R. Jia, K. Wang, Z. Zhao, H. Yang, Z. Li, Enhanced oil recovery performance and mechanism of a wormlike micelles flooding system with zwitterionic-anionic surfactants, J. Mol. Liq. 362 (2022) 119726.
[8] K. Li, X. Jing, S. He, H. Ren, B. Wei, Laboratory study displacement efficiency of viscoelastic surfactant solution in enhanced oil recovery, Energy Fuels 30 (2016) 4467–4474.
[9] A. Gbadamosi, S.M.S. Hussai, M.S. Kamal, S. Patil, T. Solling, S.F. Hassan, J. Wang, Evaluating the potential of zwitterionic surfactants for enhanced oil recovery: Effect of headgroups and unsaturation, Energy Fuels 37 (2023) 5078–5086.
[10] Y. Zhang, Y. Luo, Y. Wang, J. Zhang, Y. Feng, Single-component wormlike micellar system formed by a carboxylbetaine surfactant with C22 saturated tail, Colloids Surf. A 436 (2013) 71–79.
[11] T.M. McCoy, A. Valiakhmetova, M.J. Pottage, C.J. Garvey, L. Campo, C. Rehm, D.A. Kuryashov, R.F. Tabor, Structural evolution of wormlike micellar fluids formed by erucyl amidopropyl betaine with oil, salts, and surfactants, Langmuir 32 (2016) 12423–12433.
[12] A. Wu, Y. Gao, L. Zheng, Zwitterionic amphiphiles: Their aggregation behavior and applications, Green Chem. 21 (2019) 4290–4312.
[13] S. Lu, Q. Mei, J. Chen, Z. Wang, W. Li, C. Feng, X. Li, J. Dong, Cryo-TEM and rheological study on shear-thickening wormlike micelles of zwitterionic/anionic (AHSB/SDS) surfactants, J. Colloid Interface Sci. 608 (2022) 513–524.
[14] S. Lu, J. Dong, X. Li, Gradual transformation of anionic/zwitterionic wormlike micelles from viscous to elastic domains: Unravelling the effect of anionic surfactant chain length, J. Colloid Interface Sci. 641 (2023) 319–328.
[15] Z. Mitrinova, M. Chenkova, N. Denkov, S. Tcholakova, Cosurfactants for controlling the surface properties of diluted solutions: Interplay with bulk rheology of concentrated solutions, Colloids Surf. A 648 (2022) 129221.
[16] Z. Mitrinova, S. Tcholakova, Z. Popova, N. Denkov, B.R. Dasgupta, K.P. Ananthapadmanabhan, Efficient control of the rheological and surface properties of surfactant solutions containing C8−C18 fatty acids as cosurfactants, Langmuir 29 (2013) 8255–8265.
[17] A.P. Williams, J.P. King, A.V. Sokolova, L. Campo, R.F. Tabor, In situ nanostructural analysis of concentrated wormlike micellar fluids comprising sodium laureth sulfate and cocamidopropyl betaine using small-angle neutron scattering, Langmuir 36 (2020) 14296–14305.
[18] S. Różańska, Rheology of wormlike micelles in mixed solutions of cocoamidopropyl betaine and sodium dodecylbenzenesulfonate, Colloids Surf. A 482 (2015) 394–402.
[19] V.K. Aswal, P.S. Goyal, P. Thiyagarajan, Small-angle neutron-scattering and viscosity studies of CTAB/NaSal viscoelastic micellar solutions, J. Phys. Chem. B 102 (1998) 2469–2473.
[20] R.F. López-Santiago, J. Delgado, R. Castillo, Micellar entanglement and its relation to the elastic behavior of wormlike micelle fluids, J. Colloid Interface Sci. 626 (2022) 1015–1027.
[21] L.Y. Zakharova, E.A. Vasilieva, A.B. Mirgorodskaya, S.V. Zakharov, R.V. Pavlov, N.E. Kashapova, G.A. Gaynanova, Hydrotropes: Solubilization of nonpolar compounds and modification of surfactant solutions, J. Mol. Liq. 370 (2023) 120923.
[22] T. Liu, F. Xue, P. Yi, Z. Xia, J. Dong, X. Li, Structure-property relationship of light responsive wormlike micelles using methoxycinnamate derivatives as light switchable molecules, Acta Phys. Chim. Sin. 36 (2020) 1910004.
[23] K. Jia, J. Hu, J. Dong, X. Li, Light-responsive multillamellar vesicles in coumaric acid/alkyldimethylamine oxide binary systems: Effects of surfactant and hydrotrope structures, J. Colloid Interface Sci. 477 (2016) 156–165.
[24] R. Kumar, G.C. Kalur, L. Ziserman, D. Danino, S.R. Raghavan, Wormlike micelles of a C22-tailed zwitterionic betaine surfactant: From viscoelastic solutions to elastic gels, Langmuir 23 (2007) 12849–12856.
[25] M. Gao, P. Liu, Q. Xue, M. Zhao, X. Guo, Q. You, C. Dai, Non-ionic polar small molecules induced transition from elastic hydrogel via viscoelastic wormlike micelles to spherical micelles in zwitterionic surfactant systems, J. Mol. Liq. 359 (2022) 119343.
[26] T.M. McCoy, J.P. King, J.E. Moore, V.T. Kelleppan, A.V. Sokolova, L. Campo, M. Manohar, T.A. Darwish, R.F. Tabor, The effects of small molecule organic additives on the self-assembly and rheology of betaine wormlike micellar fluids, J. Colloid Interface Sci. 534 (2019) 518–532.
[27] S.J. Mushi, W. Kang, H. Yang, P. Wang, X. Hou, Viscoelasticity and microstructural properties of zwitterionic surfactant induced by hydroxybenzoate salt for fracturing, J. Mol. Liq. 301 (2020) 112485.
[28] S.J. Mushi, W. Kang, H. Yang, Z. Li, K. Ibrashevc, M. Issakhov, P.E. Mabeyo, Effect of aromatic acid on the rheological behaviors and microstructural mechanism of wormlike micelles in betaine surfactant, J. Mol. Liq. 332 (2021) 115908.
[29] X. Liu, Y. Cheng, X. Li, J. Dong, High-efficiency and conveniently recyclable photo-catalysts for dye degradation based on urchin-like CuO microparticle/polymer hybrid composites, Appl. Surf. Sci. 439 (2018) 784–791.
[30] T. Liu, Q. Lei, J. Dong, X. Li, Y. Lu, T. Zhou, Light-responsive vesicles based on azobenzene containing imidazolium surfactants and sodium oleate, Colloid Polym. Sci. 297 (2019) 1489–1497.
[31] T.K. Hodgdon, E.W. Kaler, Hydrotropic solutions, Curr. Opin. Colloid Interface Sci. 12 (2007) 121–128.
[32] H. Wang, B. Tan, H. Zhang, J. Wang, pH triggered self-assembly structural transition of ionic liquids in aqueous solutions: Smart use of pH-responsive additives, RSC Adv. 5 (2015) 65583–65590.

[33] Y. Lin, X. Han, J. Huang, H. Fu, C. Yu, A facile route to design pH-responsive viscoelastic wormlike micelles: Smart use of hydrotropes, J. Colloid Interface Sci. 330 (2009) 449–455.
[34] Z. Chu, Y. Feng, pH-switchable wormlike micelles, Chem. Commun. 46 (2010) 9028–9030.
[35] Z. Chu, C.A. Dreiss, Y. Feng, Smart wormlike micelles, Chem. Soc. Rev. 42 (2013) 7174–7203.
[36] Y. Feng, Z. Chu, pH-tunable wormlike micelles based on an ultra-long-chain "pseudo" gemini surfactant, Soft Matter 11 (2015) 4614–4620.